BIOLOGY OF REPRODUCTION (2012) **87**(5):115, 1–11
Published online before print 19 September 2012.
DOI 10.1095/biolreprod.112.102251

The Reproductive Phenotype of Mice Null for Transcription Factor Krüppel-Like Factor 13 Suggests Compensatory Function of Family Member Krüppel-Like Factor 9 in the Peri-Implantation Uterus[1]

Melissa E. Heard,[3] John Mark P. Pabona,[3,4] Carol Clayberger,[6] Alan M. Krensky,[6] Frank A. Simmen,[3,5] and Rosalia C.M. Simmen[2,3,4,5]

[3]*Department of Physiology & Biophysics, University of Arkansas for Medical Sciences, Little Rock, Arkansas*
[4]*Arkansas Children's Nutrition Center, University of Arkansas for Medical Sciences, Little Rock, Arkansas*
[5]*Winthrop Rockefeller Cancer Institute, University of Arkansas for Medical Sciences, Little Rock, Arkansas*
[6]*Laboratory of Cellular and Molecular Biology, National Cancer Institute, National Institutes of Health, Bethesda, Maryland*

ABSTRACT

The ovarian hormones estrogen and progesterone promote uterine receptivity and successful pregnancy through their cognate receptors functioning in concert with context-dependent nuclear coregulators. Previously, we showed that the transcription factor Krüppel-like factor (KLF) 9 is a progesterone receptor (PGR) coactivator in the uterus and that mice null for *Klf9* exhibit subfertility and reduced progesterone sensitivity. The highly related family member KLF13 displays increased expression in uteri of pregnant and nonpregnant *Klf9* null mice and similarly regulates PGR-mediated transactivation in endometrial stromal cells. However, a uterine phenotype with loss of *Klf13* has not been reported. In the present study, we demonstrate that *Klf13* deficiency in mice did not compromise female fertility and pregnancy outcome. *Klf13* null females had litter sizes, numbers of implanting embryos, uterine morphology, and ovarian steroid hormone production comparable to those of wild-type (WT) counterparts. Further, pregnant WT and *Klf13* null females at Day Postcoitum (DPC) 3.5 had similar uterine *Pgr*, estrogen receptor, and Wnt-signaling component transcript levels. Nuclear levels of KLF9 were higher in *Klf13* null than in WT uteri at DPC 3.5, albeit whole-tissue KLF9 protein and transcript levels did not differ between genotypes. The lack of a similar induction of nuclear KLF9 levels in uteri of virgin *Klf13*$^{(-/-)}$ mice relative to WT uteri was associated with lower stromal PGR expression. In differentiating human endometrial stromal cells, coincident *KLF9/KLF13* knockdown by small interfering RNA targeting reduced decidualization-associated *PRL* expression, whereas *KLF9* and *KLF13* knockdowns alone reduced transcript levels of *WNT4* and *BMP2*, respectively. Results suggest that KLF9 and KLF13 functionally compensate in peri-implantation uterus for pregnancy success.

female reproductive tract, implantation, Krüppel-like factors, pregnancy, progesterone/progesterone receptor, steroid hormone receptors

INTRODUCTION

Early pregnancy failure remains a significant health problem, with one of three human pregnancies terminating before 20 wk due to implantation defects [1]. Successful embryo implantation and development within the female reproductive tract that leads to the birth of a live young requires the endometrium and the preimplantation embryo to develop in synchrony [2, 3]. A major cause of an out-of-phase uterus resulting in reproductive failure is the dysfunctional response of endometrial stromal cells to progesterone (P_4) [4]. Working through the cognate progesterone receptor (PGR) isoforms PGR-A and PGR-B [5] in stromal cells, P_4 mediates the production of paracrine factors that allow the timely growth and differentiation of the luminal epithelium (LE) for implantation to occur. With absent or limited PGR activity (a condition known as P_4 resistance), the unopposed actions of estradiol (E_2) can disrupt the normal patterns of proliferation and compromise cell differentiation in stromal cells, leading to LE that lacks the hallmarks of an embryo-receptive state [2, 3]. Reduced, complete loss of, or altered ratios of PGR isoform expression are accepted to underlie aberrant ligand-activated PGR signaling [6–10]. Nevertheless, recognition is increasing that PGR coregulators constitute critical determinants of PGR response and that their loss of function causes misregulation of P_4-dependent signaling networks [11, 12]. To date, more than 200 proteins have been designated as PGR coregulators [13]. Thus, a key to understanding the etiology of early pregnancy failure consequent to reduced P_4 responsiveness requires the systematic elucidation of the biology and actions of these important proteins.

Our laboratory has identified Krüppel-like factor (KLF) 9 (previously known as basic transcription element-binding protein 1 [BTEB1]) as a coregulator of PGR signaling in the uterus [14, 15]. KLF9 is one of 25 currently known members of the Sp/KLF family of GC box-binding transcription factors [16, 17]. Whereas members of this family were previously thought to function simply as silencers of Sp1 transcriptional activity, KLFs have gained increased appreciation as being clinically relevant to many human pathologies by virtue of their mediation of cross-talk among signaling pathways involved in the control of cell proliferation, apoptosis, migration, and

[1]Supported by grants from the National Institutes of Child Health and Human Development HD21961 (R.C.M.S.), Arkansas Biosciences Institute/Arkansas Children's Hospital Research Institute (R.C.M.S.), Arkansas Children's Hospital Research Institute Student and Clinical Staff Intramural Program (M.E.H.), and University of Arkansas for Medical Sciences Translational Research Institute Grant UL1TR000039.
[2]Correspondence: Rosalia C.M. Simmen, Arkansas Children's Nutrition Center, 15 Children's Way, Little Rock, AR 72211.
E-mail: simmenrosalia@uams.edu

Received: 28 May 2012.
First decision: 22 June 2012.
Accepted: 19 September 2012.

eISSN: 1529-7268 http://www.biolreprod.org
ISSN: 0006-3363

differentiation, independent of Sp1 [16, 18, 19]. In the mouse uterus, KLF9 is expressed predominantly in endometrial stroma, with lower and no expression in glandular epithelium (GE) and LE, respectively [20]. KLF9 expression has been similarly reported in human endometrial stromaland GE cells during the menstrual cycle [21]. The extent to which KLF9 plays a role in uterine function was previously demonstrated from our studies of female *Klf9* null mice. We showed that *Klf9* null mutation resulted in smaller litters due to reduced numbers of implanted embryos, a shift in the normal window of embryo implantation, partial uterine P_4 resistance, and enhanced uterine estrogen sensitivity [20, 22, 23]. *Klf9* null mutation also dramatically influenced LE proliferative, apoptotic, and PGR expression status [22, 24], consistent with LE as a target of stromal KLF9 through paracrine signaling. Thus, early pregnancy loss in mice with *Klf9* null mutation likely involves disruptions of multiple early events in LE coordinated by stromal KLF9.

The KLF family members share a DNA-binding domain comprised of three zinc fingers located in the carboxyl-terminus [16, 19]. Among the KLFs, KLF9 and KLF13 exhibit the highest sequence similarities, which extend well beyond the zinc fingers [16], suggesting similar, albeit not necessarily identical, functions. In previous studies [14, 15, 25], we showed that both KLFs can transactivate the PGR-B isoform and induce PGR expression in endometrial epithelial and stromal cells in vitro. Moreover, loss of *Klf9* is accompanied by increased *Klf13* expression in nonpregnant and peri-implantation mouse uterine stromal cells [20, 25]. Because the uterine phenotype of *Klf9* null mice is subfertility rather than infertility, this finding raises the interesting possibility of regulatory and/or compensatory functions of the two KLFs in uterine endometrial cells in vivo. In the present study, we utilized mice null for *Klf13* to evaluate the contribution of this KLF to pregnancy events and to determine whether KLF9 functionally complements KLF13 in maintaining peri-implantation uterine receptivity for successful pregnancy.

MATERIALS AND METHODS

Experimental Animals

All animal experiments were conducted according to protocols approved by the University of Arkansas for Medical Sciences Institutional Animal Care and Use Committee. Animals were allowed ad libitum access to water and standard chow diet (Harlan Laboratories) and were housed in a pathogen-free barrier facility with a 12L:12D photoperiod. *Klf13*$^{(-/-)}$ mutant mice were generated by replacing exon 1 plus 0.7-kb upstream and 0.6-kb downstream regions of the *Klf13* gene with the *Neo* gene [26]. *Klf13* null mice were rederived by Charles River Laboratories before their use in our facility. Mice were genotyped by PCR of genomic DNA prepared from mouse tails as recommended by the supplier. In timed pregnancy studies, wild-type (WT) and *Klf13*$^{(-/-)}$ females of comparable ages (6–8 wk) were monitored for stage of the estrous cycle by vaginal smears and were mated at proestrus of the second estrous cycle. The presence of a vaginal plug was designated as Day Postcoitum (DPC) 0.5, and uterine tissues were collected in the morning of DPC 3.5. In studies using 8-wk-old (Postnatal Day [PND] 56) virgin mice, reproductive tissues were harvested in the morning of diestrus after the second estrous cycle.

RNA Isolation and Relative Quantitative RT-PCR

Total RNA was isolated from whole-uterine tissues (n = 4–6 mice/genotype) with TRIzol reagent (Invitrogen) following the manufacturer's protocol. RNA concentrations were determined using an ND-1000 spectrophotometer (NanoDrop Corp.). RNA (1 μg) was reverse transcribed to cDNA using iScript cDNA synthesis kit (Bio-Rad). The cDNA was diluted 1:5 (vol/vol), and 5 μl were used in a total reaction volume of 20 μl containing SYBR Green mixture (Bio-Rad) and 0.3 μM of each primer. All primers were designed to span introns using PrimerExpress software (Applied Biosystems) and synthesized by Integrated DNA Technologies, Inc. The sequences of mouse primers for real-time quantitative RT-PCR (QPCR) amplification and the amplicon sizes for each primer set are listed in Table 1. Amplification was performed under previously described thermal conditions [25] using an ABI Prism 7000 Sequence Detection System (Applied Biosystems). For each primer set, a standard curve was generated by serial dilution of pooled cDNA stocks. Quantification of individual RNAs was performed using the standard curve (hence, relative QPCR), and values were normalized to the reference gene (TATA box-binding protein [*Tbp*]).

Western Blot Analysis

Whole-cell and nuclear protein fractions from whole uteri of WT and *Klf13*$^{(-/-)}$ mice were prepared following the manufacturer's instructions (whole cell: RIPA Lysis Buffer [Santa Cruz Biotechnology]; nuclear: NE-PER [Pierce Biotechnology]), and protein concentrations were quantified by bicinchoninic acid assay (Thermo Scientific) using bovine serum albumin as standard. Whole-cell extract (100 μg) and nuclear (30–40 μg) proteins were isolated from uteri of three to four mice per genotype, separated by SDS-10% PAGE, and transferred to nitrocellulose membranes (Millipore Corp). The membranes were incubated with rabbit anti-rat KLF9 (generated in-house) at 1:1000 dilution [14] and rabbit anti-human PGR (sc-7208; Santa Cruz Biotechnology) at 1:450 dilution at 4°C overnight and further incubated with horseradish peroxidase-conjugated secondary antibody (Santa Cruz Biotechnology) for 1 h at room temperature. Immunoreactive proteins were visualized using an enhanced chemiluminescence detection system (Amersham ECL Plus; GE Healthcare Life Sciences). Membranes were stripped (Restore Western Blot Stripping Buffer; Fisher Scientific) and probed for lamin A (for nuclear proteins; Sigma) or β-actin (for whole-cell lysates; Sigma) as loading controls. Densitometric values of immunoreactive bands were quantified using the GE Image Scanner III detection system and Quantity One software (Bio-Rad).

Uterine Morphometry

Whole uteri from early pregnant (DPC 3.5) and virgin (PND 56) WT and *Klf13*$^{(-/-)}$ mice were fixed in 10% neutral buffered formalin as previously described [20]. Sections (thickness, 5 mm) were mounted on poly-L-lysine-coated slides (Fisher Scientific) and processed for hematoxylin/eosin staining following standard protocols [23, 24]. LE height was quantified using the Axiovert 200M microscope equipped with a Axiocam HRc camera and Axiovision software (Carl Zeiss, Inc.). Measurements were taken from five different fields (100× magnification) per section, and data from two to three serial sections per mouse (n = 3 mice/genotype) were analyzed.

PGR Immunohistochemistry

Formalin-fixed, paraffin-embedded uterine tissue sections from virgin (PND 56) WT and *Klf13*$^{(-/-)}$ mice (n = 3–4 mice/genotype) were prepared and incubated with rabbit anti-human PGR antibody that recognizes both PGR isoforms (sc-7208; Santa Cruz Biotechnology) at 1:300 dilution overnight at 4°C, followed by incubation with secondary antibody (Vectastain ABC kit; Vector Laboratories, Inc.) for 1 h, as previously described [22, 24]. Control sections were processed similarly, but with the omission of the primary antibody. Approximately 1000 stromal and 100 LE cells were counted, on average, from at least five to six randomly selected fields (400× magnification) per slide. For each cell type and genotype, nuclear immunopositive cells were expressed as the percentage of total cells counted ([number of nuclear-staining cells/number of total cells counted] × 100). The relative staining intensity (optical density [OD]) of PGR immunopositive cells was determined by computerized quantification using MCID Elite 7.0 software (Cambridge, Inc.). An intensity threshold was determined by scanning and averaging the intensity range of five randomly selected uterine sections from WT mice, and these values were utilized to determine the relative amount of staining for concurrent slides. Intensity values (OD) were obtained for individually stained cells and scored as 1, 2, or 3 based on the set intensity range of WT samples (3 = high staining, OD ≤ 0.299; 2 = moderate staining, 0.300 ≤ OD ≤ 0.399; 1 = light staining, OD ≥ 0.400). For each genotype, the percentage of stromal and LE cells that were assigned to each intensity category was calculated ([number of cells per scoring level/total number of scored cells] × 100). All slides were scored in a blinded fashion

Small Interfering RNA Transfections

The human endometrial stromal cell (HESC) line was propagated as previously described [25]. Transfections with small interfering (si) RNAs targeting human *KLF9* and human *KLF13* (siGeNOME SMART pool) or nontargeting (siCONTROL [*Scr*]) siRNAs (Dharmacon) were performed with Lipofectamine 2000 reagent (Invitrogen) in OPTI-MEM reduced serum-

TABLE 1. Mouse (m) and human (h) primer sequences.

Gene	Sense	Antisense	Product size (bp)
mBmp2	5′-GTACCGCAGGCACTCA-3′	5′-CCGTTTTCCCACTCATCTCT-3′	140
mcMyc	5′-TACTTGGAGGAGACATGGTGAATC-3′	5′-AGAAGCCGCTCCACATACAGT C-3′	102
mDkk1	5′-ATATCCCAGAAGAACCACACTG-3′	5′-ATCTTGGACCAGAAGTGTCTTG-3′	126
mEsr1	5′-GTCCTGCGAAGGCTGCAA-3′	5′-CCTCCGGTTCTTGTCAATGGT-3′	103
mKlf4	5′-TATGCAGGCTGTGGCAAAAC-3′	5′-ACAGCCGTCCCAGTCACAGT-3′	101
mKlf9	5′-CGTTGCCCACTGTGTGAGAA-3′	5′-TTGATCATGCTGGGATGGAA-3′	92
mKlf13	5′-TATGTGGACCACTTTGCCGCC-3′	5′-TGCTGGTTGAGGTCCGCTAGGAT-3′	203
mKremen1	5′-GTGGAAGGATGGACTGTGTAC-3′	5′-CTGATGCAGGGACTCGATG-3′	115
mLrp6	5′-TTCCAACAGTCCTTCCACAC-3′	5′-CTAGGAGCATAGTCACTGTCAC-3′	117
mNeo	5′- GATGGATTGCACGCAGGTTCT-3′	5′-AGGTAGCCGGATCAAGCGTAT-3′	375
mPgr	5′-CTAGGAGCATAGTCACTGTCAC-3′	5′-GAAAAAGCAGCCCGTCCA G-3′	197
mPgr-b	5′-GGAGATAGCGGGAGTCCTTTTT-3′	5′-GGAGATAGCGGGAGTCCTTTTT-3′	110
mTbp	5′-ACTTGACCTAAAGACCATTGCACTT-3′	5′-CAGTTGTCCGTGGCTCTCTTATT-3′	101
mWisp1	5′-AGACTGCACTGTTGGACAC-3′	5′-GGCATTGACGTTAGAGATCCG-3′	149
mWnt2	5′-AACTGCAACACCCTGGACAGAGAT-3′	5′-ATGGCGTAAACAAAGGCCGATTCC-3′	85
mWnt4	5′-GCAGTGGAGAACTGGAGAAGTGT-3′	5′-TACGCCATAGGCGATGTTGTC-3′	104
hBMP2	5′-GACGCTCTTTCAATGGACGTG-3′	5′-AGCAGCAACGCTAGAAGACAGC-3′	105
hPRL	5′-TCAACAGCTGCCACACTTCTTC-3′	5′-CATTCCAGGATCGCAATATGC-3′	114
hWNT4	5′-GTGCCAGTACCAGTTCCG-3′	5′-CACACCTGCCGAAGAGATG-3′	146

containing medium (Invitrogen) when cells were approximately 60% confluent. *KLF9* and *KLF13* siRNAs were used at 50 nM concentration, with final concentrations of siRNAs made up to 100 nM with the addition of *Scr* siRNA. Six hours after transfection, cells were washed, and medium was replaced with phenol red-free Dulbecco modified Eagle medium (Sigma-Aldrich)/2% charcoal-stripped bovine calf serum (Gemini Bio-Products). Cells were incubated for 24 h and then transferred to fresh medium containing 8-bromoadenosine-cAMP (0.5 mM), progestin (medroxyprogesterone acetate [MPA], 1 μM), and estradiol-17β (E_2, 10 nM) (all from Sigma-Aldrich) as previously described [25]. Cells were collected after 48 h of incubation and subjected to RNA expression analyses by QPCR using human primers shown in Table 1 or described previously [25]. Alkaline phosphatase (ALP) activity in HESCs transfected with control (*Scr*) or *KLF13* siRNAs was determined as previously described [25].

Radioimmunoassay

Approximately 500 μl of whole blood were collected by closed cardiac puncture from pregnant (DPC 3.5) and young adult (PND 56) WT and *Klf13*$^{(-/-)}$ mice. Serum was prepared by centrifugation at 4600 × *g* for 1 h and was stored at −20°C before analysis. Serum E_2 and P_4 levels were measured using the Ultrasensitive Estradiol RIA kit (Beckman Coulter) and the Progesterone EIA Kit (Cayman Chemical), respectively.

Statistical Analysis

Statistical analysis was performed using SigmaStat software (Version 3.5; Systat Software). For comparisons of relative QPCR, Western blot density, ALP activity, uterine morphometry, and serum steroid hormone levels, data (mean ± SEM) were evaluated for statistical significance between genotypes or treatment groups by Student *t*-test. Nuclear PGR immunostaining scores (mean ± SEM) were analyzed by two-way ANOVA followed by Tukey test. Incidence and frequency of neonatal lethality were analyzed by chi-square test. Differences were considered to be significant at $P < 0.05$.

RESULTS

Lack of a Fertility Phenotype of Klf13 Null Females

To determine if loss of *Klf13* expression affects pregnancy outcome, 6- to 10-mo-old WT, *Klf13*$^{(+/-)}$, and *Klf13*$^{(-/-)}$ females were bred with males of the same genotypes, and their litter sizes were determined. As shown in Table 2, *Klf13*$^{(-/-)}$ and *Klf13*$^{(+/-)}$ dams had numbers of pups (counted at birth) comparable to those of WT females ($P = 0.915$). *Klf13*$^{(-/-)}$ females showed no evidence of delayed labor or delivery complications previously noted in *Klf9* null mice [27]. To evaluate if the number of pups born equaled the number of embryos implanted, WT and *Klf13*$^{(-/-)}$ pregnant females (n = 8 per genotype) were euthanized postimplantation (range, DPCs 6.5–12.5), and the total numbers of embryos in both uterine horns were counted. WT females had 7.50 ± 0.75 embryos, which was not significantly different from *Klf13*$^{(-/-)}$ females (7.87 ± 0.64 embryos). Importantly, the numbers of implanting embryos and the litter size (Table 2) did not differ for each genotype (WT: $P = 0.203$; knock-out: $P = 0.205$) and between genotypes ($P > 0.05$). Females from both genotypes showed similar normal distribution of embryos within each uterine horn (Fig. 1A). The lack of gross morphological abnormalities in peri-implantation *Klf13* null uteri was further demonstrated by the histological appearance of the endometrial

TABLE 2. Litter size at birth and neonatal incidence and frequency of mortality at PNDs 1–5.

Genotype (dam)	Genotype (sire)	N[a]	Litter size	Incidence[b]	Frequency[c]
Wild type	Wild type	17	6.24 ± 1.82	0.0% (0/17)	0.0% (0/106)
Klf13$^{(+/-)}$	*Klf13*$^{(+/-)}$	13	6.31 ± 1.60	38.46% (5/13)#	20.73% (17/82)*
Klf13$^{(-/-)}$	*Klf13*$^{(-/-)}$	14	6.57 ± 1.60	92.86% (13/14)##	64.13% (59/92)**

[a] Number of litters analyzed from each mating.
[b] Litters with at least one neonatal death/total number of litters analyzed.
[c] Number of pups dead/total number of pups born from analyzed litters.
$P = 0.009$ relative to WT.
$P < 0.001$ relative to WT, $P = 0.01$ relative to *Klf13*$^{(+/-)}$.
* $P < 0.001$ relative to WT.
** $P < 0.001$ relative to WT and *Klf13*$^{(+/-)}$.

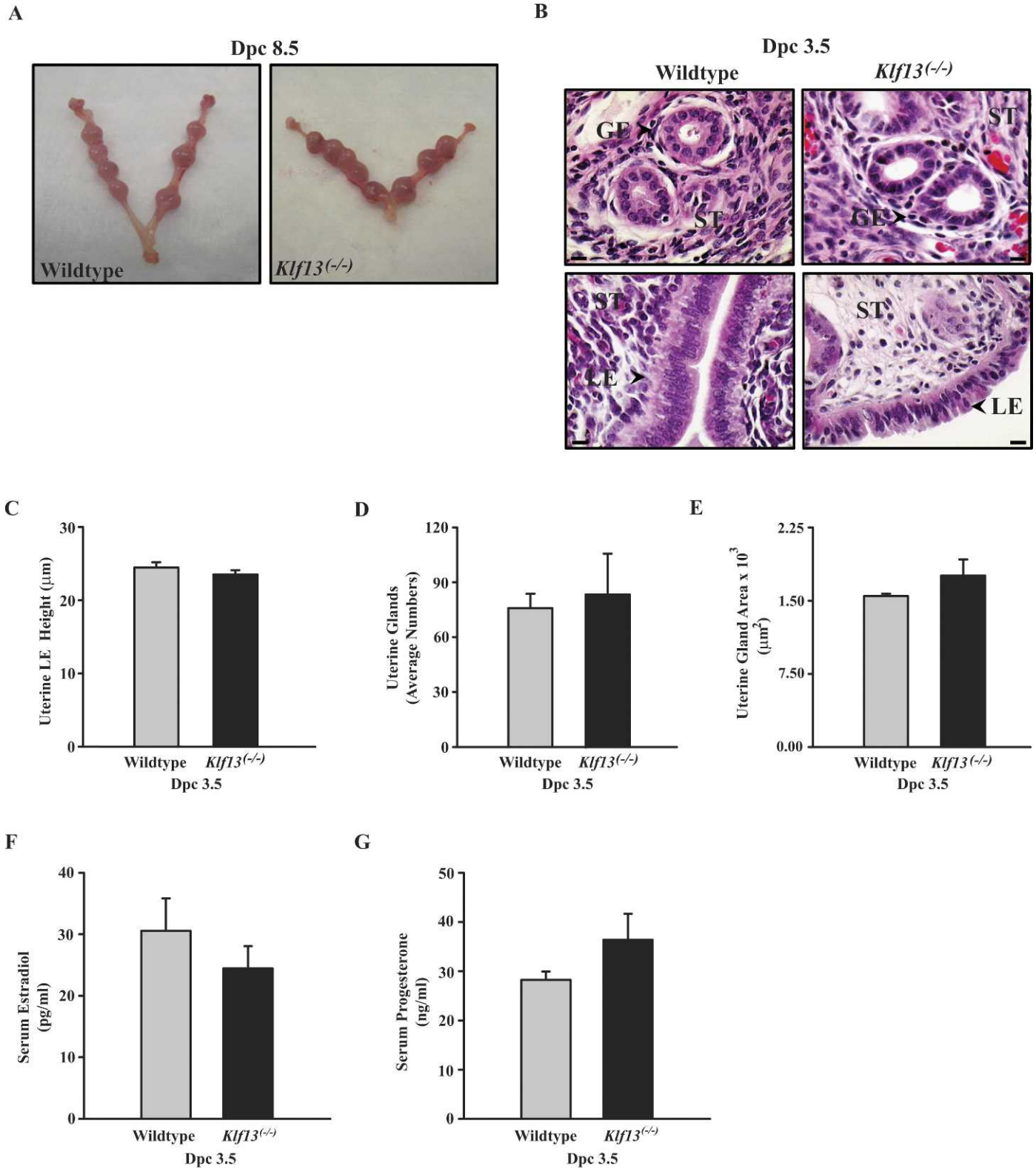

FIG. 1. Uterine phenotype and serum steroid hormone levels of *Klf13* null mice at peri-implantation. **A**) Representative images of implanted embryos in uteri of WT and *Klf13*$^{(-/-)}$ mice at DPC 8.5. **B**) Representative images of hematoxylin/eosin-stained uterine sections of WT and *Klf13*$^{(-/-)}$ mice at DPC 3.5. Each panel represents an individual mouse for each genotype. ST, stroma. Bar = 10 μm. **C**–**E**) Uterine sections from WT and *Klf13*$^{(-/-)}$ mice (n = 3 per genotype) were stained with hematoxylin/eosin and quantified for LE height (**C**), number of glands (**D**), and gland area (**E**). No differences for any uterine parameter were noted between genotypes. Data are expressed as the mean ± SEM (n = 3–4 mice/genotype). **F** and **G**) Serum E_2 (**F**) and P_4 (**G**) levels in early pregnant (DPC 3.5) WT and *Klf13*$^{(-/-)}$ females. No differences were found between genotypes for either hormone level. Data are expressed as the mean ± SEM (n = 5–7 mice/genotype).

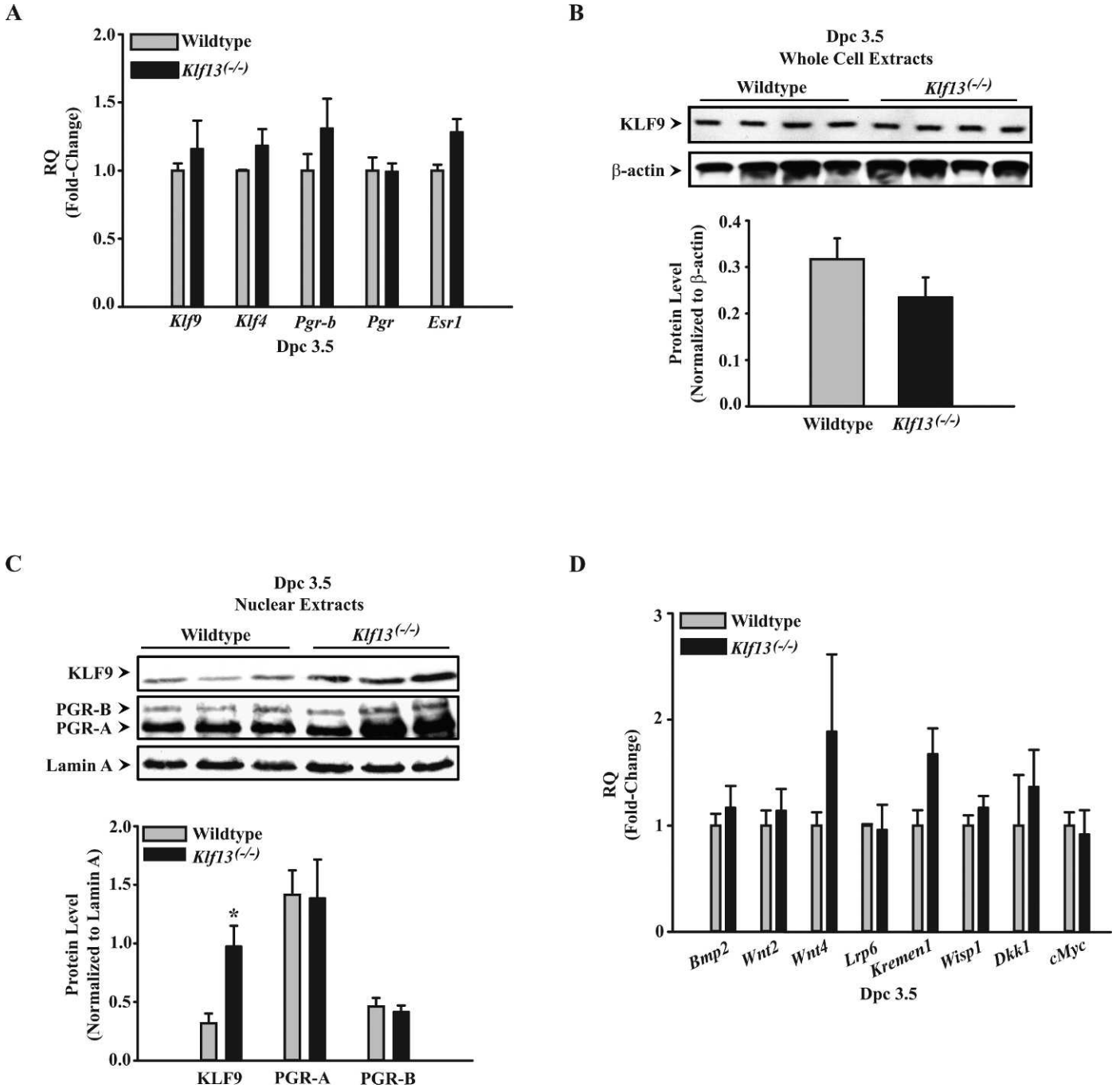

FIG. 2. Gene and protein expression in *Klf13* null uteri at peri-implantation**. A**) Messenger RNA levels of KLF family members *Klf9* and *Klf4* and of steroid hormone receptors in WT and *Klf13*$^{(-/-)}$ uteri at DPC 3.5 were quantified by relative QPCR (RQ) and normalized to those of TATA box-binding protein (*Tbp*). Data (mean ± SEM) are expressed as fold-change relative to corresponding WT uteri (n = 4–6 uteri/genotype). **B**) Western blot analyses of whole-cell extracts (100 μg of protein) from WT and *Klf13*$^{(-/-)}$ uteri at DPC 3.5 using rabbit anti-rat KLF9 and β-actin (loading control) antibodies. A representative blot (**top**) and the quantified data from densitometric scans of normalized immunoreactive bands (**bottom**) from uteri of four individual WT and *Klf13*$^{(-/-)}$ mice are shown. **C**) Western blot analyses of nuclear extracts (30 μg of protein) from WT and *Klf13*$^{(-/-)}$ uteri at DPC 3.5 using rabbit anti-rat KLF9, rabbit anti-human PGR, and anti-lamin A (loading control) antibodies. A representative blot (**top**) and the quantified data from densitometric scans of normalized immunoreactive bands (**bottom**) from uteri of three individual WT and *Klf13*$^{(-/-)}$ mice are shown. *$P < 0.05$ (Student *t*-test). **D**) Messenger RNA levels of WNT signaling-associated genes in WT and *Klf13*$^{(-/-)}$ uteri at DPC 3.5 were quantified by RQ and normalized to those of TATA box-binding protein (*Tbp*). Data (mean ± SEM) are expressed as fold-change relative to corresponding WT uteri (n = 4–6 uteri/genotype) No differences in transcript levels were found as a function of genotype.

compartments (Fig. 1B), which showed no differences in LE height, numbers of glands, and gland areas from those of WT counterparts (Fig. 1, C–E). Serum E_2 and P_4 levels in WT and *Klf13* null mice also did not differ on this day of pregnancy (Fig. 1, F and G). These results indicate that in contrast to *Klf9* null mutants [20], loss of *Klf13* in the uterus did not affect peri-implantation uterine growth, uterine receptivity to implantation, and pregnancy outcome in mice.

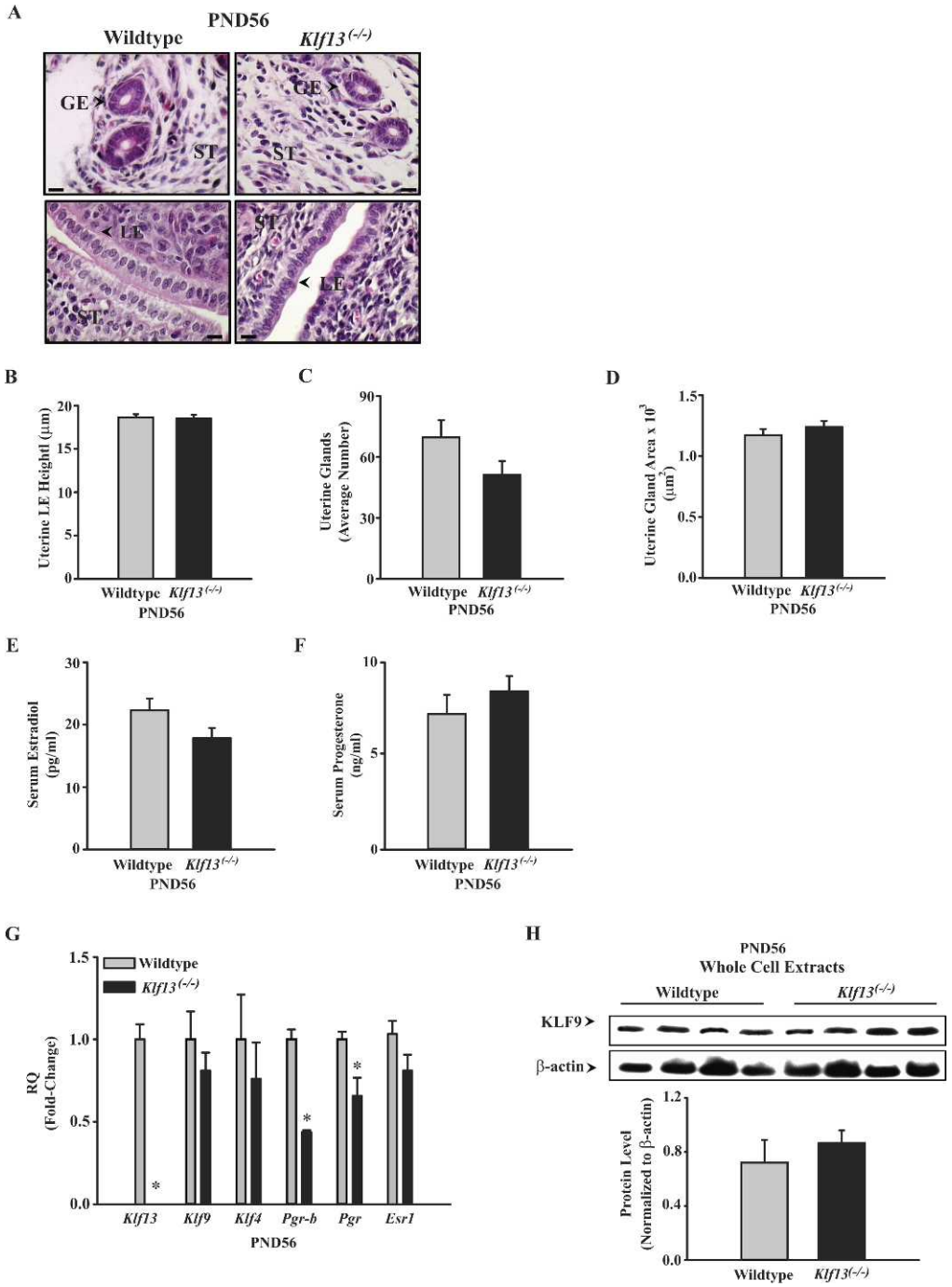

FIG. 3. Uterine phenotype, uterine gene expression, and serum steroid hormone levels of adult virgin (PND 56) *Klf13* null mice. **A**) Representative images of hematoxylin/eosin-stained uterine sections of WT and $Klf13^{(-/-)}$ mice at PND 56. Each panel represents an individual mouse for each genotype. ST, stroma. Bar = 10 µm. **B–D**) Uterine sections from (PND 56) WT and $Klf13^{(-/-)}$ mice (n = 3 per genotype) were stained with hematoxylin/eosin and quantified for LE height (**B**), number of glands (**C**), and gland area (**D**). No differences for any uterine parameter were noted between genotypes. **E** and **F**) Serum E_2 (**E**) and P_4 (**F**) levels in (PND 56) WT and $Klf13^{(-/-)}$ females. No differences were found between genotypes for either hormone levels. **G**) Messenger RNA levels of *Klf13*, *Klf9,* and *Klf4* and steroid hormone receptors in uteri of (PND 56) WT and $Klf13^{(-/-)}$ mice were quantified by relative QPCR (RQ) and normalized to those of TATA box-binding protein (*Tbp*). Data (mean ± SEM) are expressed as fold-change relative to corresponding WT uteri (n = 5–6 uteri/genotype). $^*P < 0.05$ (Student *t*-test). **H**) Western blot analyses of whole-cell extracts (100 µg of protein) from (PND 56) WT and $Klf13^{(-/-)}$ uteri using rabbit anti-rat KLF9 and β-actin (loading control) antibodies. A representative blot (**top**) and the quantified data from densitometric scans of normalized immunoreactive bands (**bottom**) from uteri of WT and $Klf13^{(-/-)}$ mice (n = 4 uteri/genotype) are shown.

Increased Neonatal Mortality with Loss of Klf13 *Expression*

The incidence and frequency of lethality within PNDs 1–5 for pups born from $Klf13^{(-/-)} \times Klf13^{(-/-)}$ mating pairs were higher than those from both $Klf13^{(+/-)} \times Klf13^{(+/-)}$ and WT × WT mating pairs (Table 2). Heterozygous $Klf13^{(+/-)}$ matings also had higher incidence and frequency of neonatal mortality than homozygous WT matings (Table 2). These results indicate that analogous to loss of *Klf9* expression,

KLF13 haplo- and total insufficiency predispose offspring to increased neonatal mortality.

Uterine Gene Expression in Early Pregnant Klf13 *Null Mice*

Our previous studies demonstrated that uterine *Klf13* mRNA and protein levels were increased in *Klf9* null females during early pregnancy [25], suggesting KLF13 compensation with KLF9 deficiency. To determine if *Klf13* null mutation similarly results in a compensatory increase in KLF9 expression in the peri-implantation (DPC 3.5) uterus that might underlie the lack of fertility loss with *Klf13* null mutation, we evaluated transcript levels of *Klf9* and its downstream target genes in uteri of WT and *Klf13*$^{(-/-)}$ mice. Relative QPCR analysis of WT and *Klf13* null uteri at DPC 3.5 showed no differences in *Klf9* and family member *Klf4* (Fig. 2A) expression. Relative gene expression levels for total *Pgr* (*Pgr-a*+ *-b*), *Pgr-b*, and *Esr1* also did not differ between the genotypes (Fig. 2A). To determine if the lack of differential expression between genotypes was likewise observed at the protein level, whole-cell lysates and nuclear extracts prepared from DPC 3.5 uteri of the two genotypes were analyzed by Western blot. KLF9 protein levels did not differ in whole-cell extracts for WT and *Klf13* null mice when normalized to the loading control β-actin (Fig. 2B). By contrast, nuclear KLF9 protein levels, normalized to lamin A as loading control, were 3-fold higher ($P = 0.029$) in peri-implantation *Klf13* null uteri than in those of corresponding WT mice (Fig. 2C). No differences in nuclear levels of PGR-A and PGR-B proteins (Fig. 2C), concordant with their respective transcripts (Fig. 2A), were observed between genotypes.

We also investigated potential changes in the expression of *Wnt* signaling components as a function of genotype, given their importance in embryo implantation [28] and our previous observation that a subset of these genes were subject to KLF9 regulation in human stromal cells [25, 29]. No significant differences in expression levels of *Bmp2*, *Wnt2*, *Wnt4*, *Lrp6*, *Kremen1*, *Wisp1, Dkk1,* or *cMyc* genes were noted between genotypes (Fig. 2D). These collective results indicate that increased nuclear KLF9 levels accompanying loss of *Klf13* expression in the peri-implantation (DPC 3.5) uteri may serve to maintain normal PGR and Wnt signaling and, thus, uterine receptivity to embryo implantation.

Uterine Gene Expression in Nonpregnant Klf13 *Null Mice*

Uteri from WT and *Klf13* null virgin (age, 8 wk; PND 56) females at diestrus were similarly evaluated for uterine morphology, histological appearance, and gene expression. Nonpregnant uteri from WT and *Klf13* null mice had comparable uterine morphology, as demonstrated by similar LE height, gland numbers, and gland sizes (Fig. 3, A–D). Uterine wet weights (relative to body weight, g/g; WT: $2.42 \pm 0.12 \times 10^{-3}$; *Klf13* null: $2.40 \pm 0.36 \times 10^{-3}$), ovarian weights (relative to body weight, g/g; WT: $4.83 \pm 0.39 \times 10^{-4}$; *Klf13* null, $5.75 \pm 0.21 \times 10^{-4}$; n = 5 mice/genotype), and serum E_2 and P_4 levels (Fig. 3, E and F) also did not differ ($P > 0.05$) between WT and *Klf13* null mice. Further, uteri from *Klf13*$^{(-/-)}$ mice demonstrated expression levels of *Klf9*, *Klf4,* and *Esr1* comparable to those from WT counterparts (Fig. 3G). The lack of differences in relative transcript levels as a function of genotype was confirmed for KLF9 protein in uterine whole-cell lysates (Fig. 3H) as well as in isolated nuclear extracts (Fig. 4A).

Interestingly, total *Pgr* and *Pgr-b* transcript levels were lower in *Klf13* null than in WT uteri (Fig. 3G). The nearly 50% decrease in *Pgr-b* gene expression with *Klf13* null mutation was confirmed for the corresponding PGR-B protein in nuclear extracts by Western blot analysis (Fig. 4A). No corresponding change was observed in PGR-A protein levels from those of WT in *Klf13* null mutants (Fig. 4A).

Analyses of uterine sections from WT and *Klf13* null mice using an anti-PGR antibody that recognizes both PGR isoforms indicated that the percentage of nuclear PGR immunopositive stromal and LE cells did not differ between WT and *Klf13* null uteri (Fig. 4, B and C). However, the percentage of nuclear cells in the stromal compartment that displayed intense anti-PGR immunostaining was lower for *Klf13* mutant than for WT uteri (Fig. 4D); conversely, a higher percentage of stromal cells was weakly immunostained for anti-PGR antibody in *Klf13* null compared to WT uteri (Fig. 4D). Interestingly, the uterine luminal compartment did not differ in the distribution of cells that strongly or weakly immunostained for anti-PGR (Fig. 4E). These results suggest that in the absence of a compensatory increase in nuclear-localized KLF9 in nonpregnant mouse uterus, a reduction in stromal PGR levels occurs with *Klf13* null mutation.

Coincident Loss of KLF9 and KLF13 Predicts Impaired Stromal Differentiation

To further evaluate a potential compensatory role of KLF9 on KLF13 function, we used siRNA targeting to knock down *KLF9* and *KLF13* mRNAs, both individually and in combination (designated siK13K9), in HESCs; control (*Scr*) siRNAs were used in parallel. Transfected cells were then incubated in medium containing 8-bromoadenosine-cAMP, MPA, and E_2 for 2 days as previously described [25] to induce decidualization and were subsequently analyzed for relative expression of well-characterized implantation/decidualization-associated genes *PRL*, *WNT4*, and *BMP2* by QPCR [25, 28, 29]. In previous studies, we showed the dramatic decrease (>90%) in KLF9 and KLF13 proteins in these cells with addition of their respective siRNAs and, importantly, that the loss of one KLF resulted in the increased expression of the other [25]. The latter finding was confirmed in the present study (Fig. 5A). Coaddition of si*KLF9* and *siKLF13* resulted in significant reductions in both *PRL* and *WNT4* transcript levels, and numerically lower transcript levels for BMP2, relative to cells expressing both KLFs (i.e., transfected with *Scr* siRNAs) (Fig. 5B). However, knockdown of *KLF9* alone significantly reduced *WNT4* but not *PRL* and *BMP2* transcript levels, whereas *KLF13* knockdown alone caused a significant reduction in *BMP2* but not *PRL* and *WNT4* transcript levels (Fig. 5B).

Alkaline phosphatase activity is a functional measure of stromal decidualization in vitro [30]. We previously showed that *KLF9* knockdown reduced ALP activity in HESCs [25]. HESCs treated with *siKLF13* under the same experimental conditions, however, did not affect ALP activity relative to control (*Scr*-transfected) cells (Fig. 5D).

DISCUSSION

In previous studies, we showed that reproduction in mice is influenced by the Sp-family member KLF9, in part, by virtue of its coregulation of PGR transcriptional activity in stromal cells [20, 22, 24, 25]. Loss of KLF9 expression in the uterus resulted in poor pregnancy outcome, uterine growth defects, partial uterine P_4 resistance, and delayed onset of parturition [20, 22, 27]. The experiments in the present study show, to our knowledge for the first time, that loss of expression of KLF9's

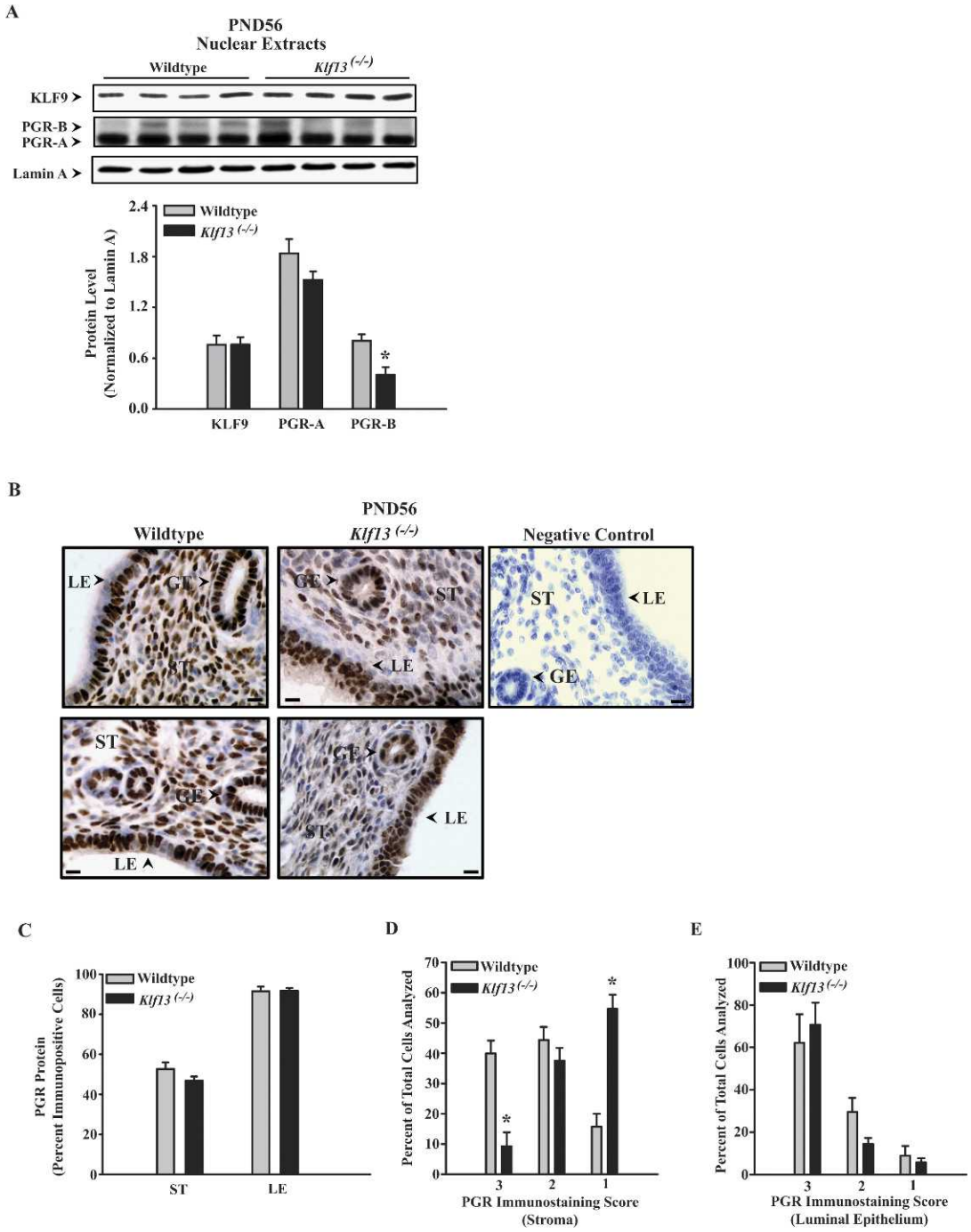

FIG. 4. KLF9 and PGR expression in uteri of adult virgin (PND 56) *Klf13* null mice. **A**) Western blot analyses of nuclear extracts (40 μg of protein) from (PND 56) WT and *Klf13*$^{(-/-)}$ uteri using rabbit anti-rat KLF9, rabbit anti-human PGR, and anti-lamin A (loading control) antibodies. A representative blot (**top**) and the quantified data from densitometric scans of normalized immunoreactive bands (**bottom**) from WT and *Klf13*$^{(-/-)}$ uteri of four individual mice are shown. *$P < 0.05$ (Student *t*-test). **B**) Representative PGR immunostaining of GE, LE, and stromal (ST) compartments in uteri of (PND 56) WT and *Klf13*$^{(-/-)}$ mice. Each panel for WT and *Klf13* knock-out mice represents a uterine section from an individual mouse. Control shows lack of immunostaining (WT uteri) in the absence of primary antibody. Original magnification, ×400; bar = 10 μm. **C**) Uterine ST and LE of (PND 56) WT and *Klf13*$^{(-/-)}$ mice were quantified for nuclear PGR immunoreactivity by determining the percentage of nuclear PGR-staining cells (mean ± SEM); three to four mice per genotype were analyzed. **D** and **E**) The percentage of uterine ST (**D**) and LE (**E**) cells in (PND 56) WT and *Klf13*$^{(-/-)}$ mice showing high (3), medium (2), and low (1) PGR immunostaining intensities were quantified, following procedures described in *Materials and Methods*. *$P < 0.05$ by two-way ANOVA followed by Tukey test.

most closely related family member, KLF13, is not critical for the maintenance of fertility in mice, most likely by virtue of KLF9's functional compensation during this period of uterine receptivity. These findings highlight the functional hierarchy of KLF9 over KLF13 in the uterus and predict, based on the in vitro results presented here using HESCs with coknockdowns of KLF9 and KLF13 relative to individual knockdowns, that the coincident loss of both KLF family members will

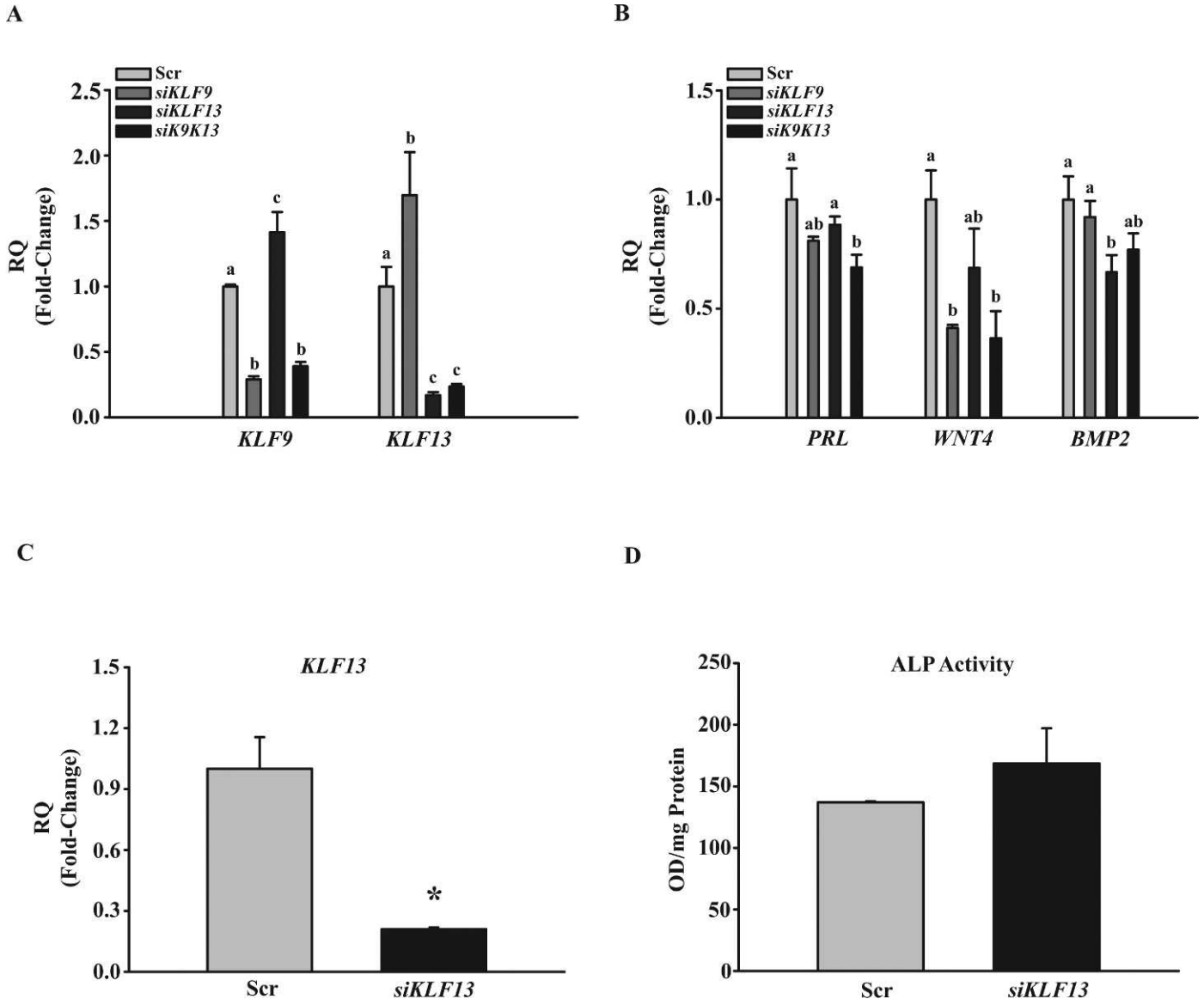

FIG. 5. Transcript levels of decidualization-associated genes with coincident *KLF9* and *KLF13* silencing. HESCs were transfected with *Scr* (control) siRNAs or siRNAs for *KLF13* and *KLF9* (50 nM each), alone and together, and treated with 8-bromoadenosine-cAMP, MPA, and E_2 for 2 days. Isolated RNAs were evaluated for transcript levels of the indicated genes by relative QPCR (RQ). **A**) *KLF9* and *KLF13* transcript levels in HESCs transfected with *KLF13* and *KLF9* siRNAs, alone or together, or with control (*Scr*) siRNAs. **B**) *PRL*, *WNT4,* and *BMP2* transcript levels in HESCs transfected with *KLF13* and *KLF9* siRNAs, alone or together, or with control (*Scr*) siRNAs. The indicated genes were quantified by RQ and normalized to those of TATA box-binding protein (*Tbp*). Data (mean ± SEM) are expressed as fold-change relative to corresponding *Scr* (control) samples. Means with different lowercase letters differed at $P < 0.05$ by one-way ANOVA followed by Tukey test. **C**) Relative *KLF13* transcript levels in control or *KLF13* siRNA transfected cells (mean ± SEM), which were analyzed for ALP activity. Values were normalized to those of TATA box-binding protein (*Tbp*) and renormalized to corresponding *Scr* (control) samples. **D**) ALP activity of cell lysates prepared from decidualizing HESCs transfected with control (*Scr*) or *KLF13* siRNAs. Data are from two independent experiments, performed in triplicates per experiment. OD, absorbance at 410 nm. *$P < 0.05$ (Student *t*-test).

significantly compromise early pregnancy events. These findings further imply that whereas KLF9 may require numerous compensatory mechanisms for its loss, one of which involves a partial KLF13 takeover [25], the compensatory mechanism for loss of uterine KLF13 may be totally dependent on KLF9. To compensate for loss of KLF13 expression and, thus, maintain PGR-B expression and transactivation of target genes, KLF9 may induce the expression of and/or increase the interaction with PGR-B as well as promote the expression and/or activity of other KLF family members, such as KLFs 3, 4, 7, and 12, all of which have been recently reported as candidate mediators of PGR function in P_4-responsive target tissues [31, 32].

The predominant loss of PGR expression in adult, cycling *Klf13* null stromal cells (which was not observed in corresponding LE cells) in the absence of an accompanying increase in nuclear KLF9 levels (as noted in early pregnant *Klf13* null uteri) is consistent with the stromal compartment being the major site of KLF9 and KLF13 expression [20, 25] and provides further support for the reliance of KLF13 on KLF9 to compensate for its function. It is therefore intriguing that we did not observe any major uterine phenotype (i.e., changes in uterine morphometry) in nonpregnant, adult *Klf13*

null mice. Although speculative, a possible explanation for this finding resides with PGR-A, which is highly expressed relative to PGR-B in the cycling adult uteri. In this regard, whereas PGR-A and PGR-B are considered to have distinct gene targets and PGR-A is considered to antagonize PGR-B signaling [33], PGR-A is critical to mouse uterine function [7, 34]. Nevertheless, it is premature to discount the contributory role of KLF13 to uterine physiology and pathology under other contexts.

Interestingly, whereas loss of KLF9 function was accompanied by increased KLF13 synthesis [25], the converse was not observed for uteri of *Klf13* null mice. The higher nuclear levels of KLF9 in *Klf13* null preimplantation (DPC 3.5) uteri, in the absence of coincident increases in transcript and total cellular protein levels, suggest enhancement of KLF9 nuclear localization and/or retention as a mechanism by which KLF9 function may be increased to ensure uterine PGR sensitivity. Like other transcription factors, the activities of numerous KLFs are regulated by their nuclear localization [35–37]. KLF family members possess one or more monopartite nuclear localization signals adjacent to or within their C-terminal DNA-binding domains and that are conserved in all KLFs [35–39]. The signal for nuclear transport or nuclear retention of KLF9 protein has not been definitively defined, but these activities may be promoted by coupling to Sin3a/b [40], similar to that recently demonstrated for KLF6 [37] or to poly(ADP-ribose) polymerase, as reported for KLF8 [41]. Further studies to evaluate the regulation of KLF9 (and KLF13) nuclear import and retention may contribute to novel mechanisms for regulating their stability and functions in pregnancy and in diseases caused by P_4 resistance.

To convincingly address the compensatory functions of KLF9 and KLF13 in pregnancy will require the generation of conditional *Klf9*/*Klf13* double-knockouts in the uterus, given the predisposition to neonatal mortality of *Klf9* [27] and *Klf13* (present study) null mice. Our results show that in decidualizing HESCs in vitro, siRNA targeting of *KLF9* alone resulted in reduced *WNT4* expression, whereas that of *KLF13* alone resulted in reduced *BMP2* expression. However, the significant attenuated expression of *PRL* with *KLF9* and *KLF13* siRNAs together, which was not observed with individual KLF knockdowns, raises the likelihood of a highly compromised uterus in vivo with coloss of these KLF members. Specifically, given the sequential expression of KLF9 and KLF13 in the pregnant uteri [25] and the role for KLF9 in the timing of uterine receptivity beginning at DPC 2.5 [22], we predict that the concurrent loss of KLF9 and KLF13 will drastically alter the timely progression of stromal and epithelial proliferation and differentiation that are requisite for embryo implantation, resulting in infertility. Nevertheless, the reduced ALP activity with loss of KLF9 expression [25], but not with loss of KLF13 expression (Fig. 5D), suggests the more prominent role of KLF9, relative to KLF13, in the peri-implantation uterus, consistent with the subfertility phenotype of the *Klf9* null mice. Whether other KLFs might also compensate for the functions of KLF9 and KLF13 is currently unknown, albeit a possibility, given recent studies suggesting a subset of KLF members serve as integrators of E_2 and P_4 signaling [31, 32, 42, 43].

A common feature of global *Klf9* and *Klf13* knockout in female mice is the lack of an ovarian phenotype. Specifically, both *Klf9* [22] and *Klf13* (present study) null females exhibit normal steroid hormone production, as evidenced by their ability to normally cycle and achieve pregnancy. Although our results are not supported by the recent report that KLF9 and KLF13 are transcriptional activators of the steroidogenic genes *LDLR*, *StAR*, and *CYP11A* in ovarian granulosa cells [44], suggesting that loss of their respective expression should lead to reduced steroidogenesis, it is possible that the KLF9-regulated gene *KLF4* [23] may take over the roles of KLF9 and KLF13 in a compensatory manner, as demonstrated for members of this family [25, 45] (present study). Alternatively, KLF9 and KLF13 may compensate for each other's function in the context of the ovary.

In conclusion, using mice null for *Klf13*, we report the existence of a compensatory function of uterine KLF9 for KLF13 during the critical window of uterine receptivity. Our studies provide a novel mechanism (i.e., increased nuclear localization/retention) by which KLF9 may take over the function of KLF13 to maintain the appropriate expression of PGR and Wnt signaling components. Given the lack of a uterine phenotype with loss of *Klf13* expression and that KLF4 is a target of KLF9 [23] but not KLF13 regulation, we propose that KLF9 occupies a higher position relative to KLF13 in the hierarchy of PGR transactivators to mediate uterine function for optimal embryo implantation.

REFERENCES

1. Edwards RG. Causes of early embryonic loss in human pregnancy. Hum Reprod 1986; 1(3):185–198.
2. Dey SK, Lim H, Das SK, Reese J, Paria BC, Daikoku T, Wang H. Molecular cues to implantation. Endocr Rev 2004; 25:341–373.
3. Matzuk MM, Lamb DJ. Genetic dissection of mammalian fertility pathways. Nat Cell Biol 2002; 4(suppl):S41–S49.
4. Psychoyos A. Hormonal control of implantation. Vitam Horm 1973; 31: 201–256.
5. Tsai M-J, O'Malley BW. Molecular mechanisms of action of steroid/thyroid receptor superfamily members. Annu Rev Biochem 1994; 63: 451–486.
6. Lydon JP, DeMayo FJ, Funk CR, Mani SK, Hughes AR, Montgomery CA Jr, Shyamala G, Conneely OM, O'Malley BW. Mice lacking progesterone receptor exhibit pleiotropic reproductive abnormalities. Genes Dev 1995; 9:2266–2278.
7. Mulac-Jericevic B, Mullinax RA, DeMayo FJ, Lydon JP, Conneely OM. Subgroup of reproductive functions of progesterone mediated by progesterone receptor-B isoform. Science 2000; 289:1751–1754.
8. Mulac-Jericevic B, Lydon JP, DeMayo FJ, Conneely OM. Defective mammary gland morphogenesis in mice lacking the progesterone receptor B isoform. Proc Natl Acad Sci U S A 2003; 100:9744–9749.
9. Burney RO, Talbi S, Hamilton AE, Vo KC, Nyegaard M, Nezhat CR, Lessey BA, Giudice LC. Gene expression analysis of endometrium reveals progesterone resistance and candidate susceptibility genes in women with endometriosis. Endocrinology 2007; 148:3814–3826.
10. Ren Y, Liu X, Ma D, Feng Y, Zhong N. Down-regulation of the progesterone receptor by the methylation of progesterone receptor gene in endometrial cancer cells. Cancer Genet Cytogenet 2007; 175(2):107–116.
11. McKenna NJ, O'Malley BW. Minireview: nuclear receptor coactivators—an update. Endocrinology 2002; 143:2461–2465.
12. Lonard DM, O'Malley BW. The expanding cosmos of nuclear receptor coactivators. Cell 2006; 125:411–414.
13. McKenna NJ, Cooney AJ, DeMayo FJ, Downes M, Glass CK, Lanz RB, Lazar MA, Mangelsdorf DJ, Moore DD, Qin J, Steffen DL, Tsai MJ, et al. Minireview: evolution of NURSA, the Nuclear Receptor Signaling Atlas. Mol Endocrinol 2009; 23:740–746.
14. Zhang D, Zhang XL, Michel FJ, Blum JL, Simmen FA, Simmen RCM. Direct interaction of the Krüppel-like family (KLF) member, BTEB1, and PR mediates progesterone responsive gene expression in endometrial epithelial cells. Endocrinology 2002; 143:62–73.
15. Zhang XL, Zhang D, Michel FJ, Blum JL, Simmen FA, Simmen RCM. Selective interactions of KLF9/BTEB1 with progesterone receptor isoforms A and B determine transcriptional activity of progesterone-responsive genes in endometrial epithelial cells. J Biol Chem 2003; 278: 21474–21482.
16. Suske G, Bruford E, Philipsen S. Mammalian SP/KLF transcription factors: bring in the family. Genomics 2005; 85:551–556.
17. Imataka H, Sogawa K, Yasumoto K, Kikuchi Y, Sasano K, Kobayashi A, Hayami M, Fujii-Kuriyama Y. Two regulatory proteins that bind to the basic transcription element (BTE), a GC box sequence in the promoter region of the rat P-4501A1 gene. EMBO J 1992; 11:3663–3671.
18. Simmen RC, Pabona JM, Velarde MC, Simmons C, Rahal O, Simmen FA.

The emerging role of Krüppel-like factors in endocrine-responsive cancers of female reproductive tissues. J Endocrinol 2010; 204(3):223–231.
19. Kaczynski J, Cook T, Urrutia R. Sp1- and Krüppel-like transcription factors. Genome Biol 2003; 4(2):206.1–206.8.
20. Simmen RCM, Eason RR, McQuown JR, Linz AL, Kang TJ, Chatman L Jr, Till SR, Fujii-Kuriyama Y, Simmen FA, Oh SP. Subfertility, uterine hypoplasia, and partial progesterone resistance in mice lacking the Krüppel-like factor 9/basic transcription element binding protein 1 (BTEB1) gene. J Biol Chem 2004; 279:29286–29294.
21. Du H, Sarno J, Taylor HS. HOXA10 inhibits Kruppel-like factor 9 expression in the human endometrial epithelium. Biol Reprod 2010; 83: 205–211.
22. Velarde MC, Geng Y, Eason RR, Simmen FA, Simmen RCM. Null mutation of Krüppel-like factor 9/basic transcription element binding protein 1 alters peri-implantation uterine development in mice. Biol Reprod 2005; 73:472–481.
23. Simmons CD, Pabona JM, Zeng Z, Velarde MC, Gaddy D, Simmen FA, Simmen RC. Response of adult mouse uterus to early disruption of estrogen receptor-alpha signaling is influenced by Krüppel-like factor 9. J Endocrinol 2010; 205(2):147–157.
24. Pabona JM, Velarde MC, Zeng Z, Simmen FA, Simmen RC. Nuclear receptor coregulator Krüppel-like factor 9 and prohibitin 2 expression in estrogen-induced epithelial cell proliferation in the mouse uterus. J Endocrinol 2009; 200:63–73.
25. Pabona JM, Zeng Z, Simmen FA, Simmen RC. Functional differentiation of uterine stromal cells involves cross-regulation between bone morphogenetic protein 2 and Krüppel-like factor (KLF) family members KLF9 and KLF13. Endocrinology 2010; 151:3396–3406.
26. Zhou M, McPherson L, Feng D, Song A, Dong C, Lyu SC, Zhou L, Shi X, Ahn YT, Wang D, Clayberger C, Krensky AM. Krüppel-like transcription factor 13 regulates T lymphocyte survival in vivo. J Immunol 2007; 178: 5496–5504.
27. Zeng Z, Velarde MC, Simmen FA, Simmen RCM. Delayed parturition and altered myometrial progesterone receptor isoform A expression in mice null for Krüppel-like factor 9. Biol Reprod 2008; 78:1029–1037.
28. Li Q, Kannan A, Wang W, Demayo FJ, Taylor RN, Bagchi MK, Bagchi IC. Bone morphogenetic protein 2 functions via a conserved signaling pathway involving Wnt4 to regulate uterine decidualization in the mouse and the human. J Biol Chem 2007; 282:31725–31732.
29. Pabona JM, Simmen FA, Nikiforov MA, Zhuang D, Shankar K, Velarde MC, Zelenko Z, Giudice LC, Simmen RC. Kruppel-like factor 9 and progesterone receptor coregulation of decidualizing endometrial stromal cells: implications for the pathogenesis of endometriosis. J Clin Endocrinol Metab 2012; 97:E376–E392.
30. Daniel SAJ, Kennedy TG. Prostaglandin E_2 enhances uterine stromal cell alkaline phosphatase activity. Prostaglandins 1987; 33:241–252.
31. Shimizu Y, Takeuchi T, Mita S, Notsu T, Mizuguchi K, Kyo S. Krüppel-like factor 4 mediates anti-proliferative effects of progesterone with G_0/G_1 arrest in human endometrial epithelial cells. J Endocrinol Invest 2010; 33: 745–750.
32. Rubel CA, Lanz RB, Kommagani R, Francl HL, Lydon JP, DeMayo FJ. Research resource: genome wide-profiling of progesterone receptor binding in the mouse uterus. Mol Endocrinol 2012; 26:1428–1442.
33. Giangrande PH, McDonnell DP. The A and B isoforms of the human progesterone receptor: two functionally different transcription factors encoded by a single gene. Recent Prog Horm Res 1999; 54:291–313.
34. Conneely OM, Mulac-Jericevik B, Lydon JP, DeMayo FJ. Reproductive functions of the progesterone receptor isoforms: lessons from knock-out mice. Mol Cell Endocrinol 2001; 179:97–108.
35. Rodríguez E, Aburjania N, Priedigkeit NM, DiFeo A, Martignetti JA. Nucleocytoplasmic localization domains regulate Krüppel-like factor 6 (KLF6) protein stability and tumor suppressor function. PLoS One 2010; 5:e12639.
36. Pandya AY, Talley LI, Frost AR, Fitzgerald TJ, Trivedi V, Chakravarthy M, Chhieng DC, Grizzle WE, Engler JA, Krontiras H, Bland KI, LoBuglio AF, et al. Nuclear localization of KLF4 is associated with an aggressive phenotype in early-stage breast cancer. Clin Cancer Res 2004; 10: 2709–2719.
37. Daftary GS, Lomberk GA, Buttar NS, Allen TW, Grzenda A, Zhang J, Zheng Y, Mathison AJ, Gada RP, Calvo E, Iovanna JL, Billadeau DD, et al. Detailed structural-functional analysis of the Krüppel-like factor 16 (KLF16) transcription factor reveals novel mechanisms for silencing Sp/KLF sites involved in metabolism and endocrinology. J Biol Chem 2012; 287:7010–7025.
38. Shields JM, Yang VW. Two potent nuclear localization signals in the gut-enriched Kruppel-like factor define a subfamily of closely related Kruppel proteins. J Biol Chem 1997; 272:18504–18507.
39. Quadrini KJ, Bieker JJ. Krüppel-like zinc fingers bind to nuclear import proteins and are required for efficient nuclear localization of erythroid Krüppel-like factor. J Biol Chem 2002; 277:32243–32252.
40. Zhang JS, Moncrieffe MC, Kaczynski J, Ellenrieder V, Prendergast FG, Urrutia R. A conserved alpha-helical motif mediates the interaction of Sp1-like transcriptional repressors with the corepressor mSin3A. Mol Cell Biol 2001; 21:5041–5049.
41. Lu H, Wang X, Li T, Urvalek AM, Yu L, Li J, Zhu J, Peng X, Zhao J. Identification of poly(ADP-ribose) polymerase-1 (PARP-1) as a novel Krüppel-like factor 8-interacting and -regulating protein. J Biol Chem 2011; 286:20335–20344.
42. Ray S, Pollard JW. KLF15 negatively regulates estrogen-induced epithelial cell proliferation by inhibition of DNA replication licensing. Proc Natl Acad Sci U S A 2012; 109:E1334–E1343.
43. Sun X, Zhang L, Xie H, Wan H, Magella B, Whitsett JA, Dey SK. Krüppel-like factor 5 (KLF5) is critical for conferring uterine receptivity to implantation. Proc Natl Acad Sci U S A 2012; 109:1145–1150.
44. Natesampillai S, Kerkvliet J, Leung PC, Veldhuis JD. Regulation of Kruppel-like factor 4, 9, and 13 genes and the steroidogenic genes LDLR, StAR, and CYP11A in ovarian granulosa cells. Am J Physiol Endocrinol Metab 2008; 294:E385–E391.
45. Eaton SA, Funnell AP, Sue N, Nicholas H, Pearson RC, Crossley M. A network of Krüppel-like Factors (Klfs). Klf8 is repressed by Klf3 and activated by Klf1 in vivo. J Biol Chem 2008; 283:26937–26947.